Theoretical Study of the Molecular Mechanism for the Oxygenation Chemistry in Rubisco

M. Oliva,[†] V. S. Safont,[†] J. Andrés,*[,†] and O. Tapia[‡]

Departament de Ciències Experimentals, Universitat Jaume I, Box 224, 12080 Castelló, Spain, and Department of Physical Chemistry, Uppsala University, Box 532, S-85121 Uppsala, Sweden

Received: March 2, 1999; In Final Form: April 23, 1999

A set of transition structures (TSs) related to the oxygenation reaction catalyzed by Rubisco is characterized theoretically. The TSs correspond to dioxygen fixation at the C2 center, hydrolysis, and C2−C3 bond breaking; reaction intermediates were found from TSs using the intrinsic reaction coordinate approach. Hydroxypropanone and 3,4-dihydroxy-2-pentanone are used as molecular models for the substrate D-ribulose-1,5-bisphosphate. Ab initio SCF MO calculations at a 3-21G and 6-31G** basis set level of theory were used; the correlation energy has been included at the MP2/6-31G** level. The set of TSs can be docked at the active site of the enzyme without steric hindrance. The geometries of the fully optimized reactants and intermediates differ to a large extent when compared with the saddle point structures. It is inferred that a molding work would be required in order to give them a molecular surface that is complementary in shape to that of the active site. A comparison of the theoretically determined transition structures and the transition state analogue 2′-carboxy-D-arabinitol 1,5-bisphosphate (CABP), whose X-ray structure at the active site is known, suggests that all aspects of the reaction pathway can be achieved without changes in volume. There is a good correspondence between the intermediates suggested by experiments and those obtained here with both molecular models. The present results represent a mechanistic alternative to the catalytic process as it is currently accepted in the literature.

1. Introduction

The most abundant protein on earth, present in green plants and photosynthetic organisms, is D-ribulose-1,5-bisphosphate carboxylase/oxygenase (Rubisco, E. C. 4.1.1.39). This protein catalyzes the initial step in Calvin's reductive pentose phosphate cycle, that is, the photosynthetic fixation of atmospheric carbon dioxide (CO_2) to Rubisco's substrate, D-ribulose-1,5-bisphosphate (RuBP). In this process, RuBP is enolized in the first step; a CO_2 molecule is then added to the C2-center of the enediol form of RuBP, yielding two molecules of 3-D-phosphoglycerate (PGA) after hydration and carbon−carbon bond cleavage processes. This process accomplishes the task of an annual fixation of 10^{11} tons of CO_2 from the atmosphere to the biosphere.[1,2] However, as discovered by Ogren[3] and confirmed by Tolbert,[4] a competing oxygenation reaction that initiates photorespiration is also catalyzed, thereby reducing the net efficiency of photosynthesis by up to 50%. In this competing reaction, dioxygen is added at the same active site, to the C2-center of the enolized RuBP, yielding phosphoglycolate as one of the oxidation products. Metabolism of phosphoglycolate produces CO_2, dissipating energy as heat. This oxygenation reaction has been considered over the years as a catalytic error of Rubisco.[5]

Although with equal concentrations of O_2 and CO_2, green plants catalyze only one oxygenation reaction per 100 carboxylation processes,[6,7] during photosynthesis, the amount of molecular oxygen in the chloroplast is 30 times larger than the amount of carbon dioxide in the medium; the oxygenation/carboxylation ratio then approaches one-third. Interestingly, some authors have claimed a positive role for the oxygenation process, saying that oxygenation can act as a defense mechanism by dissipating excess photochemical energy.[8,9] In this regard, it has been shown that plants with diminished photorespiratory capacity present severe photoinhibitions, thus providing support to the defense function hypothesis for the oxygenation process.[10,11]

The oxygenation reaction takes place, at first glance, between an organic molecule in its fundamental singlet state (enolized RuBP) and triplet O_2. For this to be possible, the presence of a cofactor or a transition metal that permits the conversion of molecular oxygen to its singlet electronic state is usually needed. However, neither a cofactor nor such a metal has been observed in Rubisco. This absence was explained when we calculated transition structures for both carboxylation and oxygenation steps.[12] The enol moiety formed by the two oxygen atoms bound to C2 and C3 (O2 and O3, respectively) were out-of-plane in the transition structures. Later, the transition structure of the intramolecular enolization step was determined. This structure displayed a nonplanar cis-like O2−C2−C3−O3 configuration.[13] The out-of-plane conformation was confirmed from X-ray data [14] obtained for the transition state analogue CABP (2′-carboxy-D-arabinitol 1,5-bisphosphate). We have shown that, with this out-of-plane conformation, singlet and triplet states of enolized RuBP may have very similar energies. Therefore, the triplet state of the substrate can combine with the dioxygen (in its fundamental triplet state) to give a supermolecule with the two electronic states energetically similar.[15,16] We explored this possibility, and previous results showed that the triplet channel is unable to explain the product formation within the catalytic process. In this work, we report on results obtained by studying the spin singlet channel, assuming that the intersystem crossing[17] had taken place just before the C2-attack. As the probability

* To whom correspondence should be addressed.
[†] Universitat Jaume I.
[‡] Uppsala University.

10.1021/jp9907342 CCC: $18.00
Published on Web 07/14/1999

SCHEME 1. Steps for the Oxygenation of RuBP Catalyzed by Rubisco, Extracted and Modified from Hartman and Harpel[40]

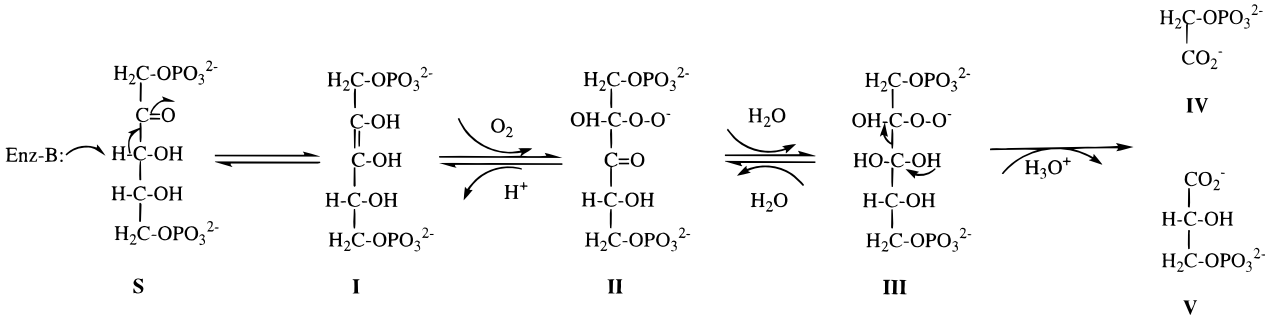

for such an event to occur is very small, the rate of oxygenation will be smaller than that of carboxylation.

From a theoretical standpoint, the oxygenation mechanism has not received much attention. Experimentally, the first concluding work on the mechanism[18] established that one of the oxygen atoms (from molecular oxygen) is incorporated into the carboxylic group of phosphoglycolate, whereas the other is lost in the medium. Furthermore, an oxygen atom is incorporated into PGA from water molecules present at the active site. From these results, a mechanistic scheme similar to that for carboxylation was proposed,[18] involving a peroxide intermediate that incorporates a water molecule, yielding an intermediate that undergoes C−C bond breaking and a final dehydration to give products (Scheme 1). This molecular mechanism is now widely accepted; however, several aspects related to it still remain unclear. (1) The inevitability postulate of Lorimer[18] indicated that the active site of Rubisco, once activated for carboxylation, was also activated for oxygenation. (2) It was unclear how the enzyme discriminates between CO_2 and O_2, although with our previous work, one might say that it is the very nature of the intersystem crossing that is responsible for such distinction. (3) A carboxyketone intermediate of the carboxylase reaction has been isolated, prompting the proposal of a corresponding peroxyketone intermediate in the oxygenase reaction.[1,19] (4) Mutants at the position of Lys 334[19] (Lys 329 in the *Rhodospirillum rubrum* sequence) are nearly devoid of carboxylation activity. Moreover, a novel O_2-dependent side product was identified for these mutant enzymes as 2-carboxytetritol 1,4-bisphosphate (CTBP). This verifies the formation of a hydroperoxide intermediate. (5) Rubisco must stabilize the peroxy intermediate for efficient cleavage of the C2−C3 and peroxyl O−O bonds. Such stabilization would cause pathways other than production of PGA and phosphoglycolate, which predominate with wild-type Rubisco, to be avoided. In mutant enzymes, however, the peroxide intermediate would be destabilized, yielding hydrogen peroxide and CTBP.[19]

The mechanistic aspects have been studied with minimal molecular models, for which transition structures can be rigorously obtained with ab initio quantum chemical techniques.[13,20−22] The study is made in the absence of any elements forming the active site, with the objective of testing whether such a complex mechanism can be sustained by minimal molecular models. Even in the absence of protein elements, the task is complex, because there is an unusually large number of chemical processes taking place in a relatively small volume. One has to describe enolization, self-inhibition, carboxylation, and all the numerous steps including hydration, carbon−carbon bond breaking, C2-inversion in carboxylation, and oxygen−oxygen bond rupture in oxygenation in order to obtain final products compatible with the experimental data. To disentangle the role of the enzyme structure from that of the chemistry that is catalyzed, we use minimal molecular models. Such an approach may help gauge the actual role of the metal and residues lining the active site. The intention is not to solve for the kinetics but to get further information on the mechanism and, in the long run, on the dynamics of the reaction (where and how the atoms move). In other words, one would like to know whether the enzyme necessarily acts as a reactant with its side chains or if the full reaction pathway can be sustained by minimal molecular models intramolecularly. In the latter case, the enzyme will act as a catalyst via productive substrate binding and thence modulation of the intrinsic mechanistic pathways. This is an issue when discussing the role of several acidic and basic groups in Rubisco. For the carboxylation reaction, we have found that a complete mechanistic pathway, describing all the complexities, can be sustained by minimal molecular models. This complexity has been found to be related to the ability of the system to carry out the chemistry using intramolecular hydrogen transfer processes.[13,20,21,23] It is important to realize that when the full enzyme representation is used, the transition structure obtained for carboxylation can be docked at the active site without steric hindrances. On the other hand, the geometrical structures of fully relaxed reactants and intermediates are not compatible with the space available at the active site. It follows, then, that substrate binding must mold the reactants into geometries compatible with the space available at the active site. This latter can be estimated from X-ray structures of enzyme−inhibitor complexes when the inhibitor is a transition state analogue.

In this paper, we explore this intramolecular route in a search for a set of transition structures that can be related to the experimental data available on this system. A preliminary report on the 3-C model was recently published.[22] The intramolecular hydrogen transfer hypothesis is further explored and applied to study the oxygenation process: the transition structures (TSs) describing the oxygenation reaction mechanism, including hydration and final C−C bond breaking, are reported, and comparisons with the experimentally accepted mechanism are discussed. The invariances of the transition structures to the level of electronic theory and model size are examined, and the possible roles of active site residues are discussed.

2. Methods and Models

2.1. Methodology. The characterization of TSs for chemical interconversion processes permits fairly clear representations of possible molecular mechanisms.[24−27] Here, the TS and structure concepts play a central role.[24,25,28−32] Practical aspects of the methodology have been previously described.[13,20,28,33]

As an extension of Pauling's lemma,[34−36] it can be assessed that for a substrate system trapped at the active site of a given enzyme and with a mechanism for an elementary step described with the help of a TS, a necessary condition to open a given

interconversion pathway is the existence of surface complementarity between the geometry associated with the TS in vacuo and at the active site. This complementarity can be checked via a geometric superposition of the calculated stationary structures with transition state analogues and slow substrates whose X-ray structure is known.

In earlier investigations, transition structures, characterized by saddle points of index one, have been determined for carboxylation, the first step in oxygenation, enolization, and self-inhibition.[12,13,15,16,20,32,33] All the calculated TSs have a remarkable property: their C-frameworks have a very small root-mean-square deviation when overlapped with the crystal structure of CABP, so that the set of TSs could also be docked at the active site.[21,22,37] This compatibility provides a plausibility argument in favor of the proposed mechanism. However, by no means are the catalytic roles of possible acidic and basic groups discarded. Their role can be discussed as shown in our later study of transition structure invariance for carboxylation, in which the QM/MM method was employed.[38] In this respect, similar studies of the whole carboxylation and oxygenation pathways are now in progress.

2.2. Models and Computing Details. A 3-C model, hydroxypropanone, and a 5-C model, 3,4-dihydroxy-2-pentanone, were selected to study the reaction mechanism. Only the two phosphate groups of the real substrate, RuBP, are missing in the 5-C model: they contribute to a productive binding as documented experimentally by X-ray studies.[14,39−43] Note that X-ray data, except for Lys 201 (carbamylated), Lys 175, Lys 334, His 327, and His 294, systematically exclude the participation of residues acting as acid/base groups because of a large distance to the substrate's atoms that are to be protonated−deprotonated.[14,43] Therefore, a model system without inclusion of external groups (to the RuBP substrate) is not a totally theoretical construct.

TSs describe theoretically well-defined geometric arrangements. The strategy followed for obtaining a TS starts by searching in the quadratic zone on the energy hypersurface in the Born−Oppenheimer approximation. Atomic displacements along the directions defined by the transition vector (TV)[44] should correspond to a zero order representation of the particular interconversion. In addition, downhill optimizations from TSs along both directions of the normal mode corresponding to the imaginary frequency were done. Those TSs that describe chemical interconversion processes would correspond to the standard TSs, whose changes may be related with experimentally based molecular mechanisms. The hypothesis that intermolecular effects will not change the nature of the TS, insofar as geometry and reaction vector fluctuation are concerned, underlies the approach used here.

The stationary points were located by optimizing the geometries at HF/3-21G and HF/6-31G** basis set levels; correlation energy has been included at the MP2/6-31G** level for the smaller model. The Berny analytical gradient optimization routines were used for the optimization.[45] The requested convergence on the density matrix was 10^{-9} atomic units; the threshold value of maximum displacement was 0.0018 Å, and that of maximum force was 0.00045 hartree/bohr. The nature of each stationary point was established by calculating analytically and diagonalizing the Hessian matrix (force constant matrix). All calculations were carried out using the GAUSSIAN 94 program.[46] Supplementary vibrational and spectral analyses were made with the AMPAC 5.0 package[47] and the GaussView 1.0 program.[48]

3. Results and Discussion

It is convenient to discuss the results by contrasting them to the existing mechanism. The experimentally-based mechanism, adapted from Hartman and Harpel,[40] is depicted in Scheme 1. The first step is the enolization of RuBP (**S**)[14,49−55] yielding the enediol intermediate (**I**), which is submitted to oxygenation via an electrophilic attack of O_2 to form the peroxyketone intermediate **II**. Hydration of **II** leads to *gem*-diol **III**. Deprotonation of one of the hydroxyl oxygens at the C3 center and dehydration of **III** is assumed to prompt for a C2−C3 bond cleavage, thus rendering the final products: one molecule of phosphoglycolate (**IV**) and one PGA molecule (**V**).

The structures calculated with the 3-C model are presented in Figure 1, which includes the atom numbering as well. They give an overview of the global process, starting from the model substrate in its enediol form (the TS for the enolization step was already reported[13]) and ending up with products. As the model substrate contains only three carbon atoms, we have checked if a more realistic model would produce a similar mechanistic pathway by using an enlarged model containing five carbon atoms. In this way, a simultaneous comparison between results obtained with the use of the two molecular models and the three theoretical levels of calculation is given in what follows so that one can appreciate structural and TV invariances to these factors.

3.1 Oxygenation TS. In Figure 2, the **TS1** for oxygenation is depicted for the two molecular models used. This stationary point describes a simultaneous addition of dioxygen to the C2 center and a hydrogen transfer between O3 and O2(O_2). This unique TS avoids proton abstraction from the substrate, thus yielding an intermediate (**I1** in Figure 1) equivalent to **II** (cf. Scheme 1) with one difference: the hydroperoxide appears protonated at the end of dioxygen addition (**I1**), so that the substrate is not overcharged. The formation of a carbonyl bond at C3 can thereafter be the object of a nucleophilic attack: the geometry is deformed, so that one may expect an activated carbonyl group at C3.

The TV associated with **TS1**, that is, the relative atom displacement phases, is represented in Figure 2 as vector displacements from the stationary geometry. Following the depicted directions, **I1** is reached; meanwhile, inverting the global sign leads to a fluctuation that overlaps the geometry of the activated reactants, **Ef** in Figure 1. This fact has been substantiated by using the Intrinsic Reaction Coordinate (IRC)[56] procedure, which permits a displacement from a given TS, following TV coordinates, to its corresponding associated minima. It is worth noticing the invariance of the TV components between the two model systems used (Figure 2a and b).

Normal mode animation of **TS1** shows the dominance of the hydrogen fluctuation: the hydrogen shifting from O3 to O2(O_2) fluctuating in antiphase with the O1(O_2)-C2 distance. The fluctuations are fully localized to this atom framework, and the imaginary frequency values show a remarkable invariance to the theoretical level and system size, ranging from 530i to 635i cm^{-1} in all studied cases.

Some distances are also included in Figure 2, which were obtained by using the different calculation levels. From the reported data, very little differences, which depend on the theoretical level used and system size can be appreciated: qualitatively, the geometric arrangement corresponds to the same structure; quantitatively, some minor variations (always less than 0.3 Å) can be found, mainly for the O1(O_2)-O2(O_2) and O1(O_2)-C2 distances. Thus, for the model systems and computational levels used, the same description is reached for this

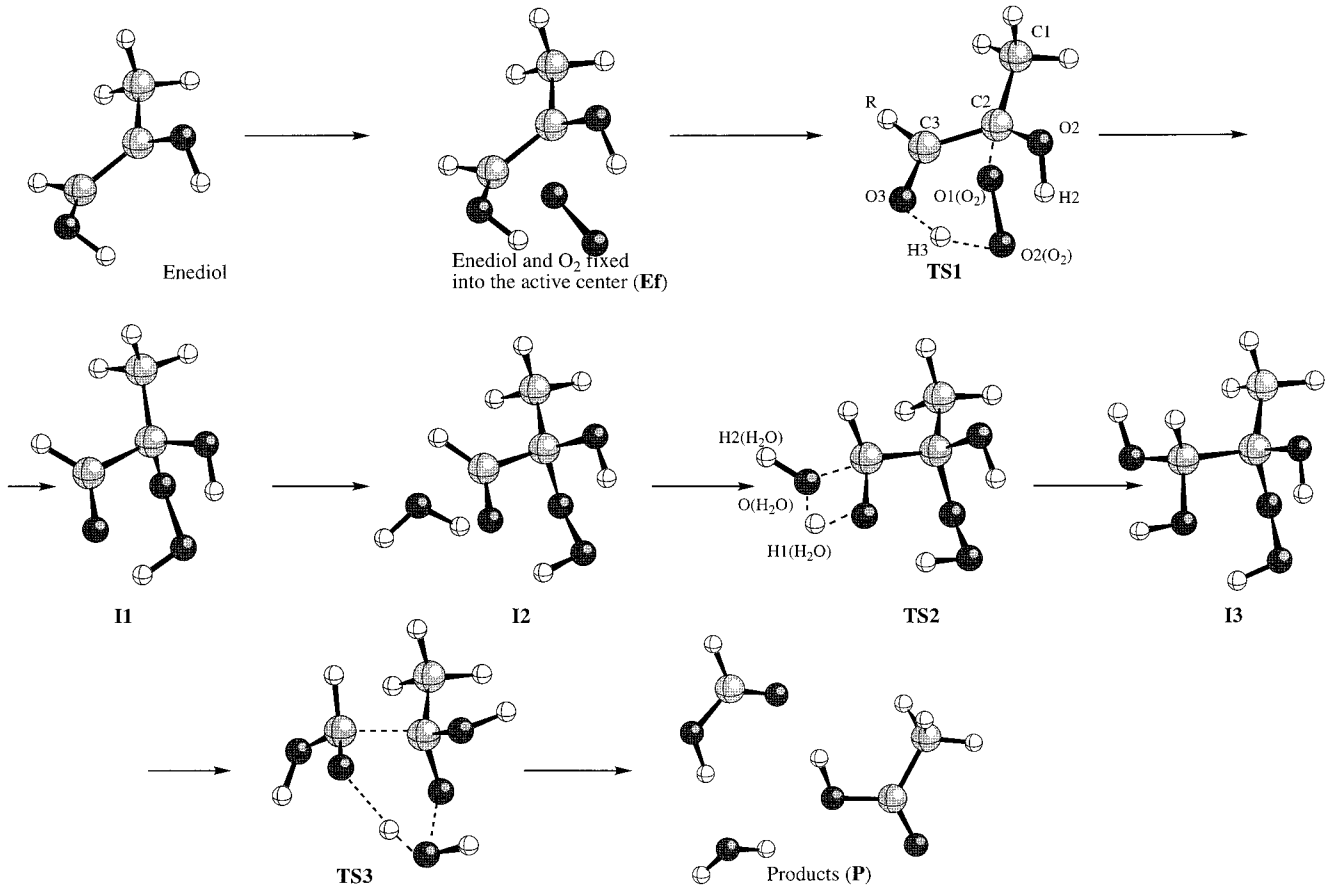

Figure 1. Schematic reaction pathways for the oxygenation obtained from ab initio calculations on a 3-C model. The atom numbering is also included.

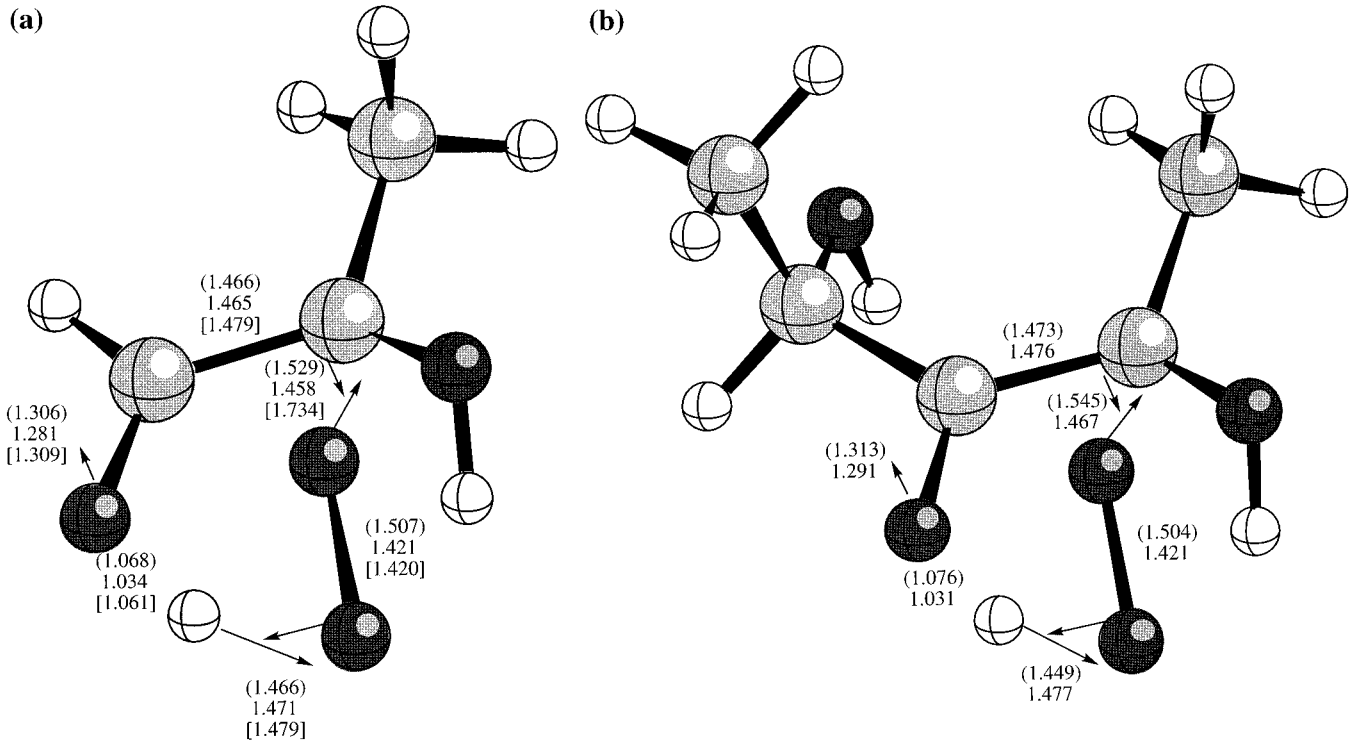

Figure 2. **TS1** for the oxygenation step: (a) 3-C model; (b) 5-C model. Main distances are indicated (Å), calculated at HF/6-31G**, HF/3-21G (in parentheses), and MP2/6-31G** (in brackets). The arrows represent the major components of the TV.

oxygenation step at a molecular level: the process can be understood as concomitant oxygen addition/hydrogen transfer processes.

Following the minimum energy path, the passage trough **TS1** would ensure the population of the reactive intermediate **I1**, which corresponds to a protonated hydroxyperoxide. As men-

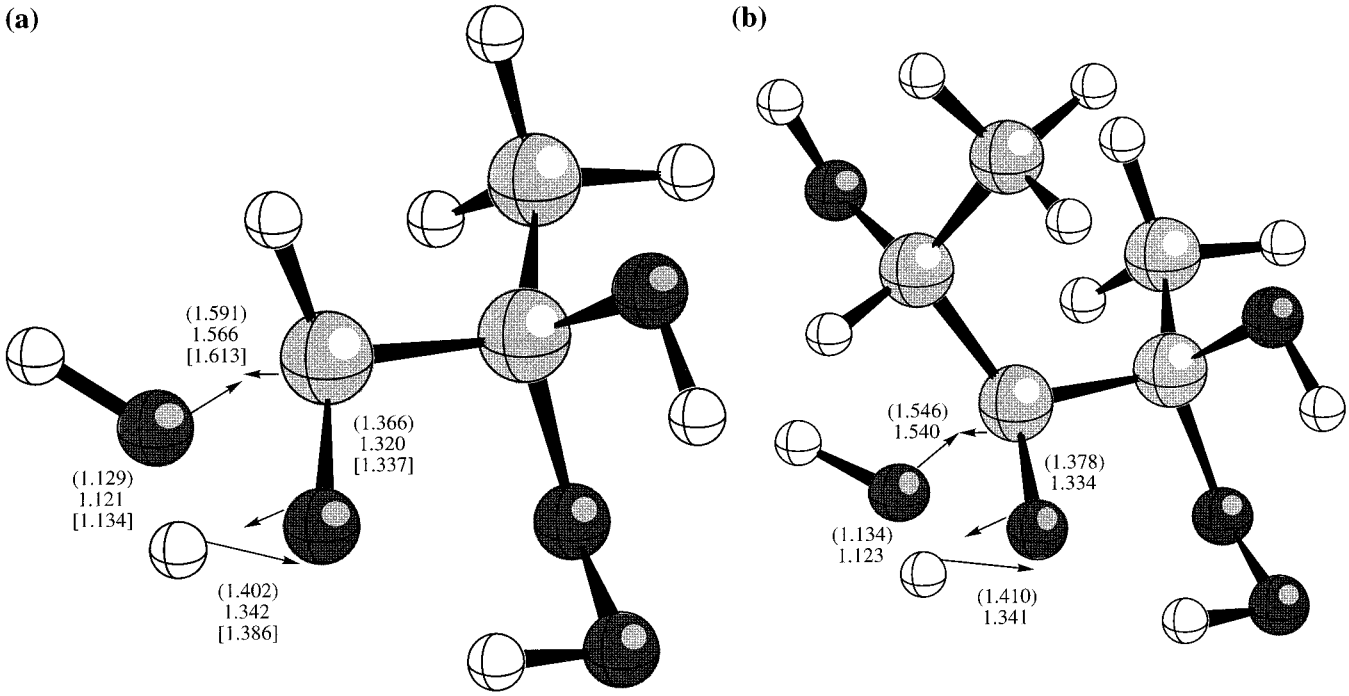

Figure 3. TS2 for the hydration process: (a) 3-C model; (b) 5-C model. Main distances are indicated (Å), calculated at HF/6-31G**, HF/3-21G (in parentheses), and MP2/6-31G** (in brackets). The arrows represent the major components of the TV.

tioned above, it differs from the species **II** proposed in Figure 1 in the sense that no proton elimination is required in our theoretical approach. Recently, Harpel *et al.*[19] have suggested that formation of CTBP, the novel O_2-dependent side product generated by a site-directed mutant, verifies the identity of Rubisco's previously invoked oxygenation intermediate as a peroxy intermediate. The existence of the stable species identified in the theoretical model (**I1**) is then in good agreement with the experimental evidence.[57] The geometry, of course, must be deformed at the active site because no space is available to geometrically relaxed reactants and intermediates.

Furthermore, the **TS1** geometry can be overlapped fairly well with CABP,[22] so that surface complementarity is ensured between the protein active site and the activated complex of the reaction catalyzed by Rubisco, as explained above.

3.2 Hydration TS. The carbonyl group of the protonated peroxide (**I1**) at C3 appears to be open for nucleophilic attack. Now, a water molecule located in the neighborhood of the coordination sphere (in the real system it is probably displaced by dioxygen binding) may initiate such nucleophilic attack at the C3-center as can be seen in the following step (**I2-TS2-I3**, see Figure 1). In the present approach, we go after a transition structure because the reactants will never be in their equilibrium geometric configuration. Again, the active site will prevent such geometric relaxation.

In Figure 3 the hydration **TS2** is depicted for both molecular models. It corresponds to a direct hydration of the carbonyl group. The related product (**I3**) is the equivalent to structure **III** in Scheme 1. This time, however, the peroxide is protonated and forms a strong hydrogen bond with the O3 oxygen. Species **I3** is a *gem*-diol structure; this kind of functionality is known to have a strong acid character that would facilitate a new intramolecular hydrogen rearrangement related to the carbon−carbon bond cleavage between C2 and C3 centers, as will be shown below.

The TV associated with **TS2** is represented in Figure 3 as vector displacements from the stationary geometry, as before. Following the IRC, the related intermediates, **I2** and **I3**, are reached from **TS2**. This means that this TS is well associated with the corresponding chemical step. It is worth noticing again the invariance of the TV components between the two model systems used (Figures 3a and 3b). From the TV components, the four center character in **TS2** is apparent: it corresponds to a concerted mechanism such that oxygen addition to C3 and proton transfer to O3 are accomplished in a single step. This type of TS has been found earlier in related hydration reactions of carbonyl compounds.[58] The **TS2** is more reactant-like in the sense that the transferred hydrogen is to the water oxygen than to O3.

Normal mode animation shows an almost fully localized fluctuation in the four center moiety, and the imaginary frequency values range from 1435i to 1858i cm^{-1}.

From the geometric data included in Figure 3, very little differences can be observed between the different theoretical levels (less than 0.07 Å), so that the invariance property can again be extended to the geometric aspects.

3.3 C2-C3 Bond Cleavage TS. The final transition structure **TS3** is depicted in Figure 4 and corresponds to a simultaneous C2−C3 and O1(O_2)-O2(O_2) bond breaking process; in addition the hydrogen of the incoming water molecule is transferred to the protonated oxygen of the peroxide, and a new water molecule is formed. Note that if a magnesium ion were present, and all the TS features were not affected by the metal, the newly formed water molecule would remain within its coordination shell. If such were the case in the real situation, this mechanism would avoid solvation−desolvation effects at the magnesium ion. At variance with the commonly accepted mechanism, the reaction, without hydronium elimination, can be accomplished simply as an intramolecular process.

The TV components describe the passage from **I3** to the products, as shown by an IRC calculation from **TS3**, and are invariant to the model size (Figures 4a and 4b) and theoretical level. The geometric data differ by less than 0.16 Å except for the MP2 results, which describe the hydrogen transfer between O3 and O2(O_2) as less developed (the hydrogen atom still remains very close to the O3 atom) and the O1(O_2)-O2(O_2) bond

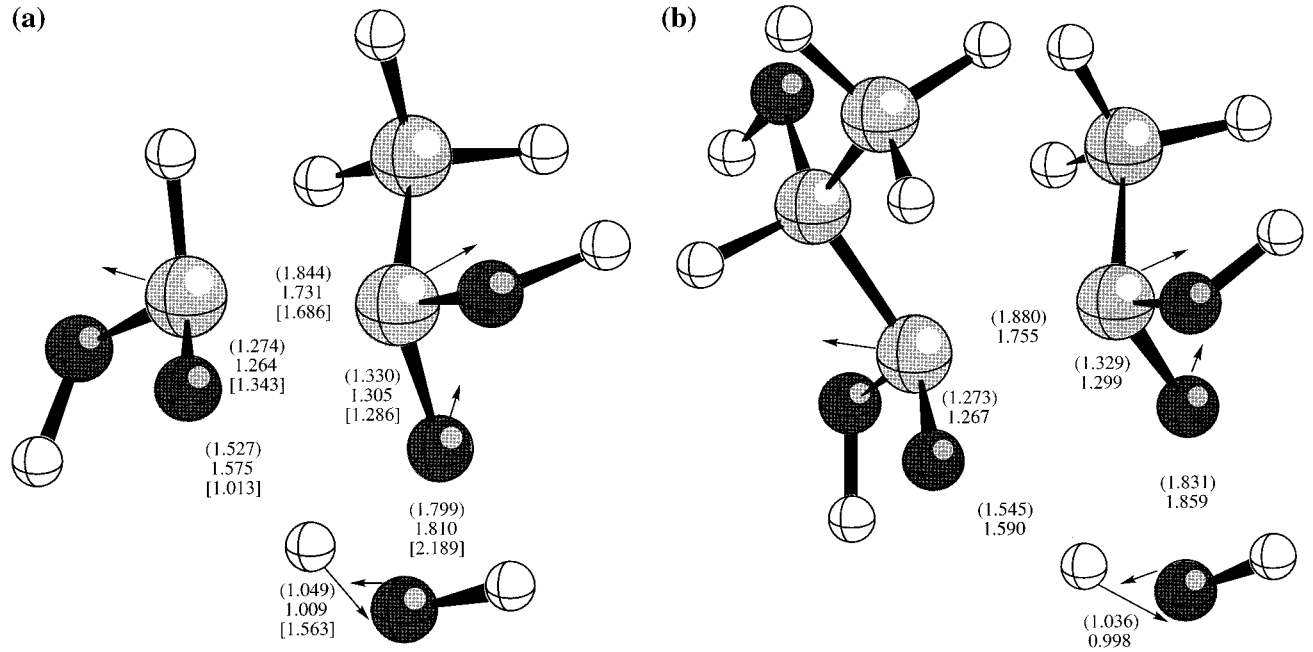

Figure 4. **TS3** for the C2−C3 bond cleavage step: (a) 3-C model; (b) 5-C model. Main distances are indicated (Å), calculated at HF/6-31G**, HF/3-21G (in parentheses), and MP2/6-31G** (in brackets). The arrows represent the major components of the TV.

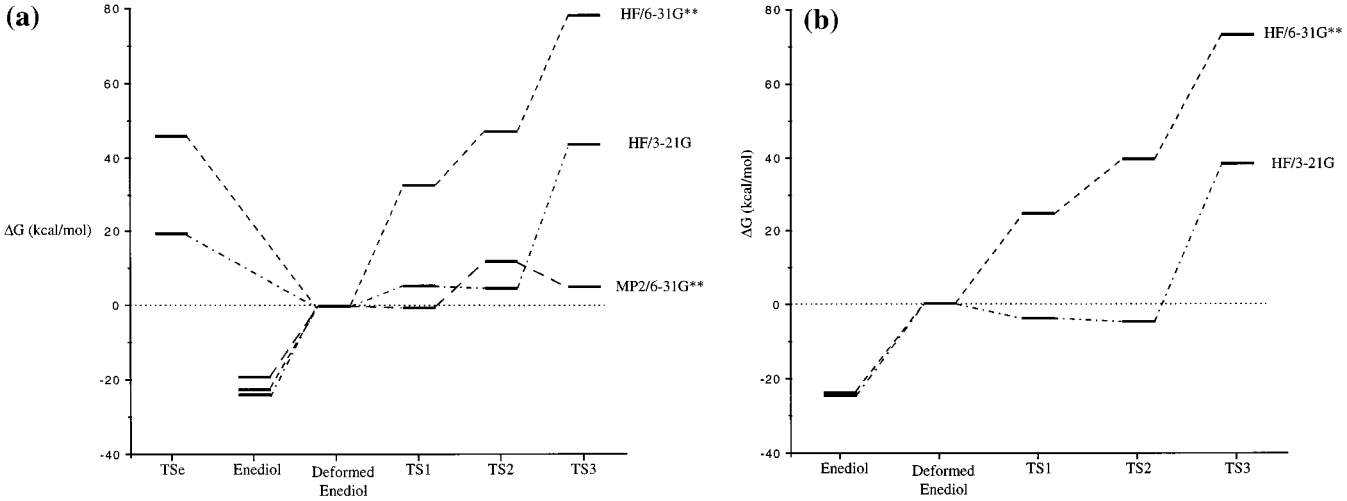

Figure 5. Free energy profile for the oxygenation pathway (from the enediol onwards) for model systems: (a) 3-C model; (b) 5-C model. TSe stands for the TS corresponding to the enolization step (not reported here; see text).

breaking as more advanced (forming a hydroxyde-like group). This difference is also reflected by a lower value for the imaginary frequency (1236i cm^{-1}), whereas for the rest of calculation methods, the values range from 1615i to 1918i cm^{-1}.

4. Final Remarks

The catalytic mechanism for oxygenation reactions has been represented with the help of a set of transition structures calculated with ab initio techniques. Intramolecular hydrogen transfer is found to be an appropriate way to accomplish the complex chemistry once the reactants are molded into the geometries characteristic of the TSs. This self-consistency was also found for TSs calculated for carboxylation, for intramolecular hydrogen transfer leading to enolization, for self-inhibitory pathways, and for oxygenation.[13,15,16,20,21,32,33] The introduction of the intramolecular enolization mechanism[13] was the key to obtaining a more economic mechanistic description. The corresponding TSs also gave some clues in explaining the slow inactivation of the enzyme observed in vitro, and possibly in vivo; this slow inactivation can be qualitatively understood in terms of stereochemically incorrect intramolecular retro-enolization processes.[20] Moreover, TSs for the hydrolytic step that follows carboxylation and the inversion of configuration of products at the C2-center were determined.[21,23] Here, we present a study, which complements and completes a previous letter,[22] in which all TSs related to the oxygenation−hydrolysis path are characterized on model compounds that represent the real substrate of Rubisco; the TSs are fully consistent with present experimental data and have the essential group elements that intervene in the chemistry of this system.

As noted before, the carbon and oxygen frame of **TS1** for dioxygen addition, determined in a vacuum, can be overlayed with CABP bound to the active site of Rubisco as observed in the X-ray structure.[14,22] This superposition demonstrates the surface complementarity needed for the mechanism described by using TSs calculated in a vacuum to have catalytic significance according to Pauling's lemma.[34−36] We note that phosphate binding is critical to obtain a correct geometry for

the substrate. A crystal structure of activated Rubisco with its substrate obtained by Lundqvist and Schneider[59] shows a significant difference at the phosphate binding site when compared with the CABP complex. The crystal has no catalytic activity. In view of the stringent geometric constraints set up by the transition structure, which geometrically overlays with CABP, one may conjecture that a fine-tuned substrate binding is required for catalysis.

Structurally, all TSs share the gross conformational characteristics (see Figure 1) and therefore can be docked without steric hindrances at the Rubisco active site when the latter is correctly activated. The interesting result is that both the oxygenation and carboxylation chemistry, insofar as transition structures are concerned, can be accomplished without the help of external proton donor−acceptor groups. Of course, such a reaction in vacuo is not achievable because of the large geometric deformation required and the too-large activation energies. One of the important roles of the enzyme would be, according to this perspective, to fix the substrate in a conformation suitable for the reaction. Productive binding is then evident. A second point requiring further study is to establish the role of the magnesium ion and its coordination shell and whether the intramolecular hydrogen interconversion can or cannot be accomplished. Preliminary results show that this mechanism survives as theoretically expected.[26,60]

The structural invariance of the TS has also been tested when different wave functions and molecular models are used. This result is reinforced by our recent QM/MM study,[38] in which 3493 atoms were considered classically and 29 plus a water molecule in the quantum subspace. The structure of the saddle point of index one found is very similar to the one calculated in vacuo. To what extent the arguments given about TS invariances are wishful thinking or, on the contrary, express something meaningful, is a key problem not only to warrant the working hypothesis used by us, but also to make more precise the way one looks at reaction pathways in physical and general chemistry. To go from one transition structure to another, these species must have finite lifetimes.

A caveat is in place here concerning the nature of the conclusions with respect to the real system. In theory, the model seems to indicate that the chemistry of Rubisco can be achieved in the absence of acid−base catalysis by active site side chains. In reality, there is much more to enzyme catalysis, as Fersht's work on tRNA synthethases[61] and many others have shown. For Rubisco, we have discussed above some of the complexities. The transition structures in vacuo are to be considered as molecules having a finite lifetime. To achieve a mechanistic path, defined by a TS, the enzyme must prompt for an adequate population of their vibrational states. The kinetics may be totally controlled by those factors, making possible events such as a loop closing motion. It is then wrong to conclude, on a more or less dogmatic overtone, that the only role of active site residues is to stabilize transition states. One of the roles emerging from calculations and comparisons with X-ray data is that the protein must mold the reactants and must add sufficient energy to them so that they can populate the vibrational states of the TS.

A very approximate idea of the job expected from the enzyme in lowering the energy barriers by molding the reactants can be obtained from the Born−Oppenheimer free energy values for the calculated TSs relative to the enediol deformed in a geometry compatible with the active site. These free energy values are presented in Figure 5 for the different molecular models and theoretical levels of calculation. As one can expect, the results are dependent on these factors. The energetic results must be taken only as rough approximations, because a sound evaluation of energetics must take into account the multiple interactions between the substrate and the enzyme residues at the active center: this will be the goal of future studies on the whole process using the QM/MM methodology. At any rate, from the results given, one can see that about 20 kcal/mol is needed to mold the enediol reactant. It is interesting to see how the obtained tendencies are invariant to the model size, although they are very dependent on the calculation level. In this respect, our best calculation, at MP2/6-31G**, shows a very smooth profile once the enediol is deformed: only about 12 kcal/mol would be needed to get the highest energy TS in this case. It is here, then, where the active site residues may increase the catalytic efficiency by lowering the energies of the transition structures relative to the precursor and succesor complexes.

Acknowledgment. This work was supported by research funds provided by the Ministerio de Educación y Ciencia, DGICYT (Project PB96-0795-C02-02). Calculations were performed on two Silicon Graphics Indigo2 Impact R10000 workstations of the Departament de Ciències Experimentals and on two Silicon Graphics Power Challenge L of the Servei d'Informàtica of the Universitat Jaume I. We are indebted to these centers for providing us with computer capabilities. M.O. thanks the Ministerio de Educación y Ciencia for a FPI fellowship. O.T. thanks NFR (Swedish Natural Sciences Research Council) for financial support.

References and Notes

(1) Miziorko, H. M.; Lorimer, G. H. *Annu. Rev. Biochem.* **1983**, *52*, 507.
(2) Schneider, G.; Lindqvist, Y.; Brändén, C.-I. *Annu. Rev. Biophys. Biomol. Struct.* **1992**, *21*, 119.
(3) Bowes, G.; Ogren, W. L.; Hagerman, R. H. *Biochem. Biophys. Res. Commun.* **1971**, *45*, 716.
(4) Lorimer, G. H.; Andrews, T. J.; Tolbert, N. E. *Biochemistry* **1973**, *12*, 18.
(5) Andrews, T. J.; Morell, M. K.; Kane, H. J.; Paul, K.; Quinlan, G. A.; Edmonson, D. L. In *Carbon Dioxide Fixation and Reduction in Biological and Model Systems*; Oxford University Press: Oxford, 1994.
(6) Jordan, D. B.; Ogren, W. L. *Nature* **1981**, *291*, 513.
(7) Andrews, T. J.; Lorimer, G. H. *J. Biol. Chem.* **1985**, *260*, 4632.
(8) Powles, S. B.; Osmond, C. B. *Plant. Physiol.* **1979**, *64*, 982.
(9) Kozaki, A.; Takeba, G. *Nature* **1996**, *384*, 557.
(10) Wu, J.; Neimanis, S.; Heber, U. *Bot. Acta* **1991**, *104*, 283.
(11) Heber, U.; Bligny, R.; Streb, P.; Douce, R. *Bot. Acta* **1996**, *109*, 307.
(12) Tapia, O.; Andres, J. *Mol. Eng.* **1992**, *2*, 37.
(13) Tapia, O.; Andrés, J.; Safont, V. S. *J. Phys. Chem.* **1994**, *98*, 4821.
(14) Andersson, I. *J. Mol. Biol.* **1996**, *259*, 160.
(15) Andrés, J.; Safont, V. S.; Tapia, O. *Chem. Phys. Lett.* **1992**, *198*, 515.
(16) Andrés, J.; Safont, V. S.; Queralt, J.; Tapia, O. *J. Phys. Chem.* **1993**, *97*, 7888.
(17) Shaik, S. S. *J. Am. Chem. Soc.* **1979**, *101*, 3184.
(18) Lorimer, G. H.; Andrews, T. J. *Nature* **1973**, *248*, 359.
(19) Harpel, M. R.; Serpersu, E.; Lamerdin, J. A.; Huang, Z.-H.; Gage, D. A.; Hartman, F. C. *Biochemistry* **1995**, *34*, 11296.
(20) Tapia, O.; Andres, J.; Safont, V. S. *J. Phys. Chem.* **1996**, *100*, 8543.
(21) Safont, V. S.; Oliva, M.; Andrés, J.; Tapia, O. *Chem. Phys. Lett.* **1997**, *278*, 291.
(22) Oliva, M.; Safont, V. S.; Andrés, J.; Tapia, O. *Chem. Phys. Lett.* **1998**, *294*, 87.
(23) Oliva, M.; Safont, V. S.; Andrés, J.; Tapia, O. *J. Phys. Chem. A* **1998**, submitted.
(24) Houk, K. N.; Gustafson, S. M.; Black, K. A. *J. Am. Chem. Soc.* **1992**, *114*, 8565.
(25) Williams, I. H. *Chem. Soc. Rev.* **1993**, 277.
(26) Tapia, O.; Paulino, M.; Stamato, F. M. L. G. *Mol. Eng.* **1994**, *3*, 377.
(27) Houk, K. N.; González, J.; Li, Y. *Acc. Chem. Res.* **1995**, *28*, 81.
(28) Tapia, O.; Andres, J. *Chem. Phys. Lett.* **1984**, *109*, 471.
(29) Wolfenden, R.; Radzicka, A. *Curr. Opin. Struct. Biol.* **1991**, *1*, 780.

(30) Miller, W. H. *Acc. Chem. Res.* **1993**, *26*, 174.
(31) Albery, W. J. *Adv. Phys. Org. Chem.* **1993**, *28*, 139.
(32) Tapia, O.; Andrés, J.; Safont, V. S. *J. Mol. Struct. (THEOCHEM)* **1995**, *342*, 131.
(33) Tapia, O.; Andrés, J.; Safont, V. S. *J. Chem. Soc., Faraday Trans.* **1994**, *90*, 2365.
(34) Pauling, L. *Chem. Eng. News* **1946**, *24*, 1375.
(35) Pauling, L. *Nature* **1948**, *161*, 707.
(36) Pauling, L. *Am. Sci.* **1948**, *36*, 51.
(37) Andrés, J.; Oliva, M.; Safont, V. S.; Moliner, V.; Tapia, O. *Theor. Chem. Acc.* **1999**, *101*, 234.
(38) Moliner, V.; Andrés, J.; Oliva, M.; Safont, V. S.; Tapia, O. *Theor. Chem. Acc.* **1999**, *101*, 228.
(39) Andrews, T. J.; Lorimer, G. H. In *The Biochemistry of Plants*; Hatch, M. D., Boardman, N. K., Eds.; Academic Press: New York, 1987; Vol. 10, p 131.
(40) Hartman, F. C.; Harpel, M. R. *Annu. Rev. Biochem.* **1994**, *63*, 197.
(41) Knight, S.; Andersson, I.; Brändén, C.-I. *J. Mol. Biol.* **1990**, *215*, 113.
(42) Gutteridge, S.; Rhoades, D.; Herrmann *J. Biol. Chem.* **1993**, *268*, 7818.
(43) Andersson, I.; Knight, S.; Schneider, G.; Lindqvist, Y.; Lundqvist, T.; Brändén, C.-I.; Lorimer, G. H. *Nature* **1989**, *337*, 229.
(44) McIver Jr., J. W. *Acc. Chem. Res.* **1974**, *7*, 72.
(45) Schlegel, H. B. *J. Chem. Phys.* **1982**, *77*, 3676.
(46) Frisch, M. J.; Trucks, G. W.; Schlegel, H. B.; Gill, P. M. W.; Johnson, B. G.; Robb, M. A.; Cheeseman, J. R.; Keith, T.; Peterson, G. A.; Montgomery, J. A.; Raghavachari, K.; Al-Laham, M. A.; Zakrzewski, V. G.; Ortiz, J. V.; Foresman, J. B.; Cioslowski, J.; Stefanov, B. B.; Nanayakkara, A.; Challacombe, M.; Peng, C. Y.; Ayala, P. Y.; Chen, W.; Wong, M. W.; Andres, J. L.; Replogle, E. S.; Gomperts, R.; Martin, R. L.; Fox, D. J.; Binkley, J. S.; Defrees, D. J.; Baker, J.; Stewart, J. P.; Head-Gordon, M.; Gonzalez, C.; Pople, J. A. *GAUSSIAN 94*, Revision B.1; Gaussian, Inc.: Pittsburgh, PA., 1995.
(47) *Ampac 5.0*; Semichem: Shawnee, KS, 1994.
(48) *GaussView 1.0*; Gaussian, Inc.: Pittsburgh, PA, 1997.
(49) Saver, B. G.; Knowles, J. R. *Biochemistry* **1982**, *21*, 5398.
(50) Sue, J. M.; Knowles, J. R. *Biochemistry* **1982**, *21*, 5410.
(51) Hartman, F. C.; Soper, T. S.; Niyogi, S. K.; Mural, R. J.; Foote, R. S.; Mitra, S.; Lee, E. H.; Machanoff, R.; Larimer, W. F. *J. Biol. Chem.* **1987**, *262*, 3496.
(52) Lorimer, G. H.; Hartman, F. C. *J. Biol. Chem.* **1988**, *263*, 6468.
(53) Smith, H. B.; Larimer, F. W.; Hartman, F. C. *Biochem. Biophys. Res. Commun.* **1988**, *152*, 579.
(54) Schloss, J. V. In *Enzymatic and Model Carboxylation and Reduction Reactions for Carbon Dioxide Utilization*; Aresta, M., Schloss, J. V., Eds.: Kluwer Academic Publishers: Dordrecht, The Netherlands, 1990; p 321.
(55) Newman, J.; Gutteridge, S. *J. Biol. Chem.* **1993**, *268*, 25876.
(56) Fukui, K. *J. Phys. Chem.* **1970**, *74*, 4161.
(57) Chen, Y.-R.; Hartman, F. C. *J. Biol. Chem.* **1995**, *270*, 11741.
(58) Spangler, D.; Williams, I. H.; Maggiora, G. M. *J. Comput.Chem.* **1983**, *4*, 524.
(59) Lundqvist, T.; Schneider, G. *J. Biol. Chem.* **1991**, *266*, 12604.
(60) Tapia, O.; Andres, J.; Stamato, F. M. G. In *Solvent Effects and Chemical Reactivity*; Tapia, O., Bertran, J., Eds.; Kluwer: Dordrecht, 1996; p 283.
(61) Fersht, A. *Enzyme Structure and Mechanism*, 2nd ed.; W. H. Freeman & Co.: New York, 1985; p 475.